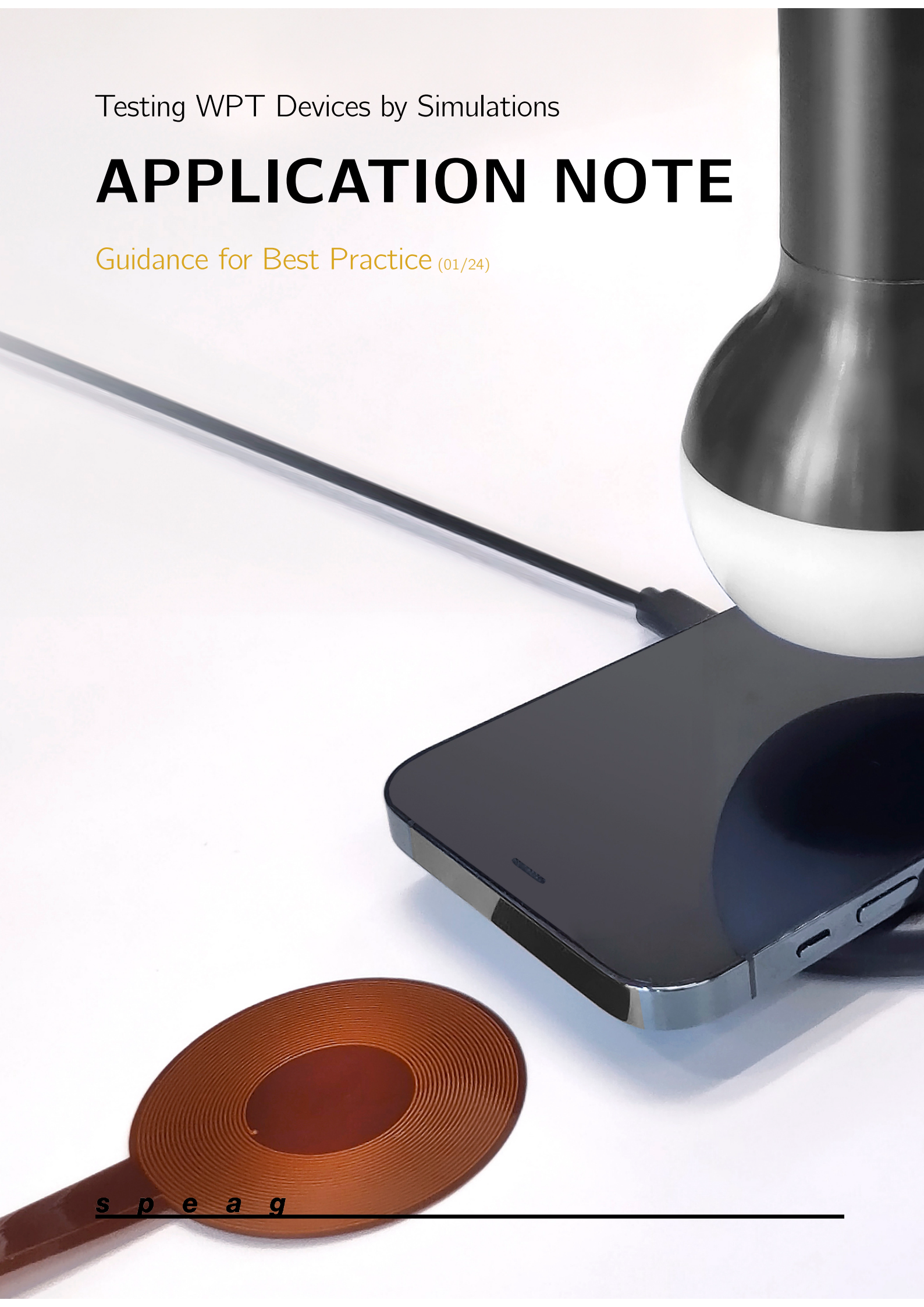


Testing WPT Devices by Simulations

APPLICATION NOTE

Guidance for Best Practice (01/24)



Testing Compliance of WPT Devices by Simulations: Best Practice

Executive Summary

This document provides basic guidance on how to demonstrate compliance of inductive wireless power transfer (WPT) systems, including the development of a computational model for the device under test (DUT), thorough validation of the model, and the determination of the uncertainty of the evaluation appropriate for near-field conditions. The process is illustrated with an example evaluation.

It is shown that the magneto quasi-static solvers are suited for inductive solvers provided it can be experimentally demonstrated that the incident electric (E-) field can be neglected.

The uncertainty budget is dominated by the validation uncertainty due to the near-field properties of WPT sources. It is also demonstrated that validation at larger distances, e.g., 20 mm above the location of closest exposure ultimately has large uncertainties because the source characteristics are lost at these larger distances, i.e., the fields of many typical sources are very similar at larger distances, whereas the exposure at close distances can differ significantly. Evaluations with an uncertainty of <3 dB are possible when the most advanced instrumentation for validation is used. However, the uncertainty ($k = 2$) will exceed 10 dB for common non-gradient magnetic field probes that are often several centimeters in diameter, and can exceed 20 dB for probes with a diameter of 5 cm.

1 Scope of this Document

The current draft of the International Electrotechnical Commission (IEC) on methods for assessing exposure to wireless power transfer (WPT) systems (IEC 63184) [1] accepts the demonstration of compliance of inductive WPT devices based on numerical simulations. IEC 63184 requires that the numerical model of the WPT device under test (DUT) be validated experimentally and that the overall uncertainty of the demonstration of compliance be determined. It is regarded as good practice to insure that the total uncertainty, which also includes the uncertainty of the experimental validation of the DUT model, does not exceed 2 dB.

Several national regulatory bodies extend the specifications of IEC 63184 [1] with additional guidelines. Among these are the Innovation, Science and Economic Development (ISED) Canada document ISED SPR-002, Issue 2 [2] and the US Federal Communications (FCC) document KDB 680106 D01 V04 [3]. These guidelines, however, still lack guidance, in particular, with respect to the comprehensive assessment of uncertainties. The objective of this document is to provide basic guidance on how to develop the computational model of the DUT, to validate the model, and to determine a comprehensive uncertainty budget.

2 Description of the Problem

For compliance evaluation of inductive and resonant WPT systems, the incident magnetic (H-) field has to be regarded as the predominant source of exposure. In general, the H-field decays steeply with distance d from the DUT (see Figure 1.1, but the actual decay rate depends heavily on the coil design, the location on the surface of the DUT with respect to the coil, and the objects that cover the transmitter, e.g., the receiver, whose coils also

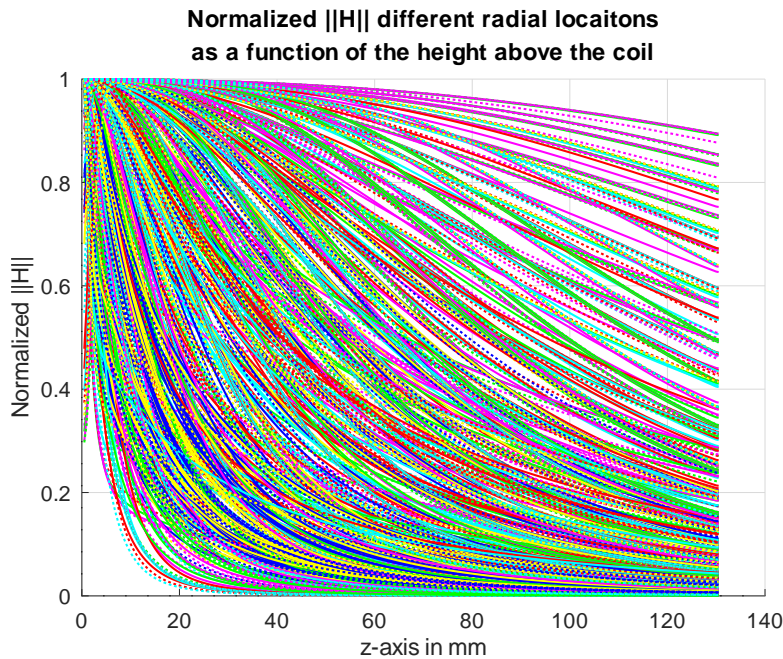


Figure 1.1: Normalized H-fields of 70 generic WPT coils without receivers. When normalized to a given distance, the variation is >20 dB for similar distributions.

contribute to the overall H-field.

In the case of inductive WPT systems, the field impedance, i.e., the ratio of $\|E\|/\|H\|$ is low, i.e., $\ll 377 \Omega$, and the fields induced by the H-field in the standard phantom [4] or in anatomical models, e.g., in those of the Virtual Population (VIP) [5], can be determined by full-wave or quasi-static solvers.

The focus of the model validation is on the evaluation of the incident fields to which the user is exposed, i.e., it is required that the simulated fields be compared to measured values on several lines in space starting from the closest accessible location. In many cases, this is the surface of the DUT. At larger distances (e.g., at 30 mm), the fields and their gradients are very similar for different source configurations and largely different exposures and are, therefore, not suitable for validation of exposure, as the resulting uncertainties would be >10 dB.

However, reasonably small error bounds can be achieved only when probes with small sensors (≤ 10 mm) are applied for the validation measurements, especially when these probes also provide information on the gradient of the field. For validations performed at larger distances, an uncertainty propagation model must be established. As the field gradients at larger distances are only very poorly correlated to the gradients close to the DUT, the uncertainty generally increases to several dBs (Appendix B) and represents the dominant factor in the model uncertainty and eventually in the overall uncertainty budget of the compliance assessment.

The DUT may also cause significant exposure of the tissues of the user to electric (E-) fields. In the case of inductive WPT systems operating at <4 MHz, these E-fields are generally caused by the accumulation of charge on the small conductive surfaces/edges or at tuning capacitors. These fields, which are not directly associated with the H-field, depend heavily on the design and manufacturing details of the DUT, e.g., on surface shape, materials and construction, placement of components, wiring or tracks on the circuit board, etc. The E-fields decay much faster than the H-fields, with rates of up to $1/d^4$ at close distances to the source [6], are very difficult to simulate, and nearly impossible to validate. Solutions are provided in this document and in [7].

The non-homogeneity of the tissues in the human body can cause local enhancements of the induced E-field when compared to a homogeneous standard phantom. As these enhancements are only local, they hardly affect the spatial peak specific absorption rate (SAR) values (psSAR_{1g/10g}). In [8], coverage factors for the E-field

enhancement were determined statistically on the basis of approximately 3500 simulations. These coverage factors are conservative for all exposure situations. The most common approach for the quantification of human exposure is to test compliance with these coverage factors applied to the assessment with the standard phantom. Lower exposure enhancement with respect to the flat phantom may be determined for specific use cases by performing a similar study as in [8], with only the exposure scenarios that are relevant for the specific case taken into consideration. Nevertheless, the difficulty of such a study is the simulation of a number of scenarios that is sufficiently large to provide a solid statistical assessment of the coverage factor.

3 Workflow of the Compliance Testing Procedure

3.1 Selection of Solvers

As the first step, the most adequate solver for the problem must be chosen. The criteria for the selection of the solver, with the pros and cons of each, are given in Appendix A. The main criteria for the selection of the solver are:

- the operation frequency of the DUT is within the quasi-static limits (Appendix A.2)
- the exposure induced by the incident E-fields of the DUT is negligible in comparison to the H-field exposure

If both conditions are fulfilled, the simulations can be carried out with the magneto quasistatic (MQS) solver. Otherwise, a fullwave solver, e.g., a finite-difference time-domain (FDTD) or finite element method (FEM) solver, must be applied. See Appendix A.3 for a detailed comparison of the properties of the different numerical solvers and Appendix C for a demonstration of the validity of the approach. A flowchart of this and the following steps is given in Figure 1.2.

3.2 Exposure Scenarios

3.2.1 General

Exposure to the H-fields of the DUT can be conservatively assessed with the standard phantom and the coverage factors derived in [8]. As a less conservative approach, a representative set of anatomical body models [5] can be evaluated in typical and worst-case positions with respect to the DUT.

Because of the high gradients of both the incident E- and the H-fields, the phantom or the body models must be positioned as close as possible to the DUT. For magnetic coupling, the highest exposure occurs when the mutual inductance between the coil and the exposed body is maximized, i.e., when the coil is in the coronal position with respect to a large flat area of the body, such as the chest [9, 10]. For electric coupling, the maximum exposure can be assumed when the E-field is concentrated at a small region of the body, e.g., when the finger tips are placed next to an electrode tip or a tuning capacitor [6].

The configuration of the DUT model has to take both the transmitter and the receiver into account, as well as their impacts on the incident fields. Details on the test conditions are given in [11].

3.2.2 Conservative Approach with the Standard Phantom and Coverage Factors

The standard phantom is specified in [1]. The elliptical phantom of [4] or, alternatively, a phantom with rectangular shape that reproduces the conditions of an exposed person may be used. Such a phantom, filled with a homogeneous tissue simulating liquid (TSL) having a relative permittivity $\epsilon_r = 56$ and a conductivity $\sigma = 0.75 \text{ S/m}$, is specified in [1] for the frequency range 4 MHz to 30 MHz. According to the approach of [8], the exposure assessed with the flat phantom is converted by means of the coverage factors for comparison with the respective basic restrictions. These coverage factors are applicable over the frequency range 1 kHz to 10 MHz.

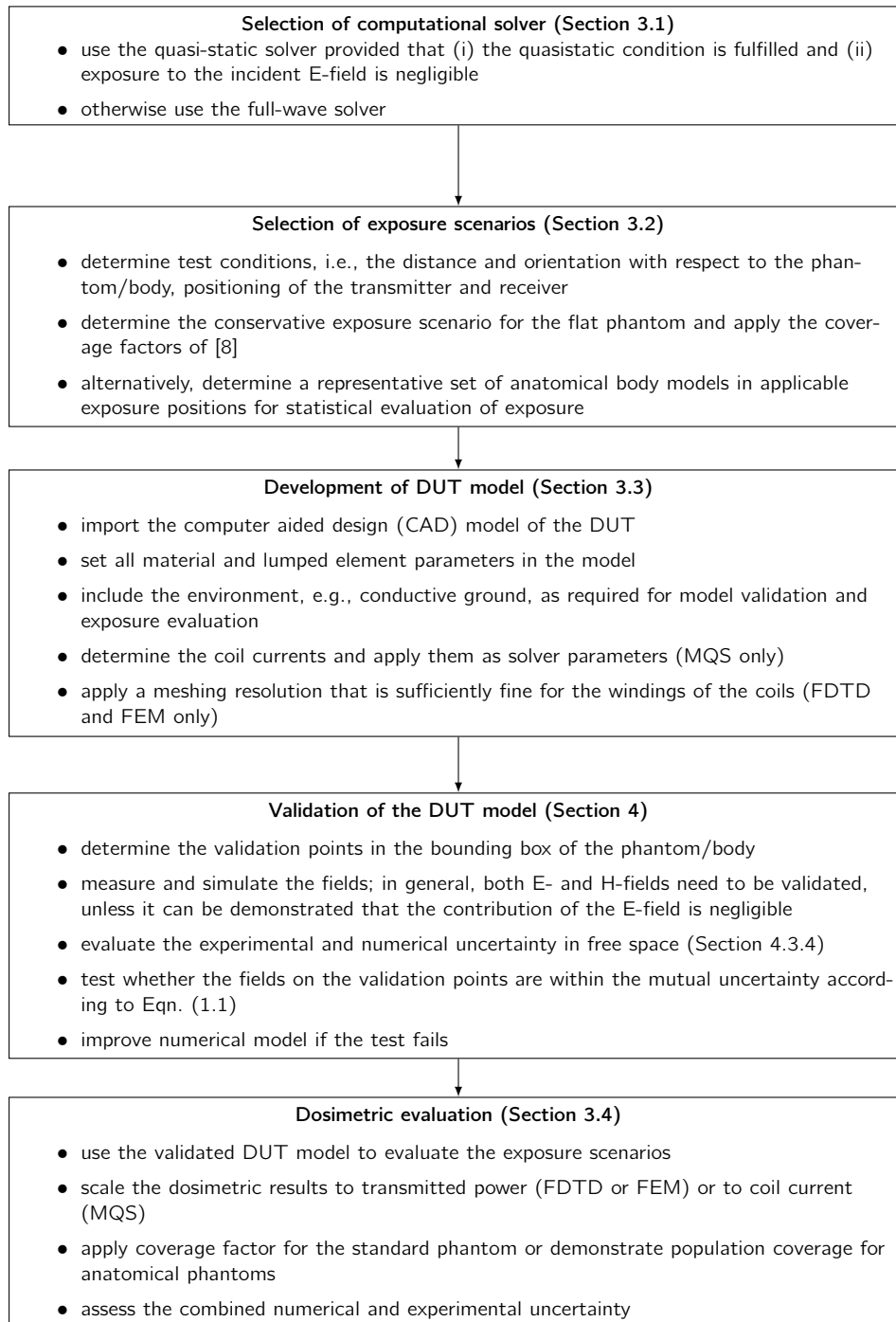


Figure 1.2: Workflow of the numerical compliance evaluation.

3.2.3 Modeling Particular Exposure Scenarios with Anatomical Models

The evaluation of the exposure in terms of basic restrictions performed with the standard phantom (Section 3.2.2) may yield an overly conservative result. The use of anatomical models of the human body [5] to evaluate the exposure of a particular population group in representative exposure scenarios, e.g., for particular postures and distances from the DUT, can be expected to reduce the level of conservativeness.

The exposure scenarios should be selected on the basis of the accessibility of the device. Portable or desk mounted devices positioned close to the body may expose any part of the body, including the limbs, the torso when bent over the device, or the head, e.g., when the user falls asleep at the desk where the device is mounted. Examples can be found in [10]. Wireless vehicle chargers may not expose the entire body, because the presence of the vehicle restricts how a person can approach the coils while the vehicle is being charged. Nevertheless, a person could reach under the car, thereby positioning hands close to the coils. Small children may be able to crawl under a car with high clearance and risk being exposed.

It should be noted that the assessment of the exposure of a particularly exposed population group may require the evaluation of at least several hundred configurations for coverage to be statistically relevant. The algorithms for the assessment of the basic restrictions specified in [1, 12, 13] can be used to directly evaluate exposures in the anatomical models.

3.3 Development of the DUT Model

The development of the computational model of the DUT should be based on the original CAD model provided by the manufacturer. Both transmitter and receiver must be represented in the model, as well as the currents induced in the receive coil. Metal parts in the environment of the WPT system, such as the body of a vehicle and the dielectric or conductive ground, as well as ferrite shielding, must be included if the fields of the WPT system are altered by their presence. Dielectric parts, e.g., of the casing of the DUT can have an impact on the E-fields of the DUT. These must be included in the model if exposure to the incident E-field is relevant. Annex H.2.2 [1] gives general guidance on the modeling regarding the H-field exposure. Additional considerations and requirements are summarized below:

- **Model parts:** The numerical model of the DUT should be based on its original CAD data and must include both the transmitter and the receiver. As the impact of the parts of the model on the fields is generally not known beforehand, all parts of the CAD model must be included.
- **Dielectric materials:** Dielectric materials, which impact the E-field distribution, must be included. If these parameters are not specified in the documentation of the device, they must be derived from database values or, preferably, based on measurements and must be considered for model validation and uncertainty assessment (Sections 5.2 and 5.2).
- **Coil models and feedlines:** The DUT model must appropriately account for the discretization of the windings of the transmit and receive coils, and their feedlines, as the latter may also conduct substantial currents.
- **Conduction losses:** Dielectric and metallic losses in conducting parts can generally be assumed to be negligible at frequencies of up to 30 MHz.
- **Ferrites:** Ferrite materials must be included in the model. Properties that are not provided with the documentation of the device must be based on assumptions and are subject to model validation and uncertainty assessment (Sections 4 and 5.2). If the DUT contains ferrite materials, the Biot-Savart solver cannot be applied to calculate the incident H-field.
- **Source and load:** The DUT model can be fed by a single lumped source placed on a mesh edge when FDTD or FEM solvers are used. Matching networks may need to be included. If the receive coil is modeled, a lumped resistance should be connected to its terminals to simulate the load. When the Biot-Savart-solver or the MQS-solver is used, the source and the loading of the receive coil cannot be modeled by lumped sources. The coil currents must be specified directly on the conducting elements and be determined by measurements beforehand.

- **Lumped elements:** Lumped elements can be integrated into an FDTD model to simulate capacitors, inductors, or resistors required for tuning or loading the model if the components they replace do not contribute to exposure. Like the sources in the FDTD model, the lumped elements operate on a single grid edge and can be connected directly to the conducting parts of the model. As the spatial dimensions of the lumped elements in the mesh may differ from the dimensions of the real components, the field distribution around a lumped element will be different from the field distribution of the DUT.

Note: Lumped elements may be used only when it can be demonstrated that they do not contribute to exposure.

3.4 Dosimetric Evaluation

After successful validation according to Section 4, the dosimetric analysis can be carried out according to the workflow described in Section 3.2. The computational algorithms for the extraction of the dosimetric quantities are specified in [1, 12, 13]. The results are scaled to the transmitted power (FDTD or FEM) or the coil current (MQS), and the coverage factors are used for the evaluation [8] when the standard phantom is used; when the coverage of the exposed population must be demonstrated for the dosimetric results, anatomical models are used. The results must be reported together with the combined numerical and experimental uncertainty as described in Section 5.2.

4 Validation of the DUT Model

4.1 General

The validation of the DUT model demonstrates that its incident fields correspond to those of the original device within the known uncertainty bounds. The incident fields must be evaluated experimentally, and the validation needs to include the incident field maxima in the regions that are accessible to the user given the large field gradients that are common for WPT devices (Section 2). At present, the specification of the validation procedure of IEC 63184 [1] is still under revision, and the extended specifications of [2, 3] require additional details concerning robust validation of the model.

This application note provides detailed instructions to validate the DUT model developed (Section 3.3) based on the experimental and computational evaluation at a set of points that comprise the relevant characteristics of the incident field (Section 4.2). For the validation, the uncertainty of the simulation parameters (Section 4.3.1), the properties of the DUT model (Section 4.3.2), and the measurements (Section 4.3.3) are quantified. The respective sections provide the necessary guidance in addition to the specifications of the current draft of [1].

Note: If the exposure of the DUT E-field is assessed, both the E-field and the H-field of the DUT model must be validated according to the procedures described in Sections 4.2 to 4.5.

4.2 Validation Points of the Incident Field

The procedure to determine the validation points for the comparison of the measured and simulated fields is the same for both the E- and the H-fields. The points are chosen as follows:

- Determine the bounding box of the phantom with respect to the DUT: in general, the bounding box should touch the case of the DUT such that the overall field maximum is captured.
- Determine the H-field maximum anywhere on the bounding box; this maximum will serve as a reference point for the validation points described below.
- Determine the E-field maximum anywhere on the bounding box; this maximum serve as a reference point for the validation points described below.

- Determine four additional points around the point of the field maximum, to form the corner points of a square with the field maximum in its center. The edges of the square are aligned to the edges of the bounding box and have a length of approximately 40% of the mean diameter of the coil. The length of the lines is the mean diameter of the coil. At least 3 points are distributed on each of the lines equidistantly with step sizes of 10 – 20 mm. The validation locations can also be assessed on the basis of the simulation results.
- In the case of multiple local maxima within 3 dB of the absolute maximum, repeat the procedure above to determine additional validation points. Additional local maxima due to symmetries of the coil or the DUT model need not be evaluated separately.

4.3 Uncertainty Evaluation for the Model Validation

4.3.1 Numerical Uncertainties of the Incident E- and H-Fields

The numerical uncertainties of the incident E- and H-fields, which include the contributions of the parameters and settings of the numerical solver, are evaluated according to Table 1.1. Guidance on the evaluation of the uncertainty components is given below:

- 1. Mesh resolution:** The mesh resolution uncertainty is evaluated according to Clause 9.3.2 of [1]. Additionally, the impact of the discretization of the coil windings should be considered when a full wave method – or any quasistatic method that does not include calculation of the incident field with a Biot-Savart solver – is used. In these methods, the currents in the windings are represented by the H-fields that surround them. For the independent representation of the currents in parallel windings, at least two voxels (FDTD) or tetrahedra (FEM) are required. The impact of discretization of the space between the coil currents with two to four voxels or tetrahedra is evaluated and included in the uncertainty of the mesh resolution unless the coils are discretized with a finer resolution in the default mesh.
- 2. Location of evaluation points within the mesh:** The validation points (Section 4.2) do not always coincide with the boundaries of a meshing element and may, therefore, be subject to interpolation uncertainties, which are evaluated by quantifying the difference at adjacent mesh points based on non-interpolated data of the computational grid.
- 3. Convergence:** When the MQS-solver or an FEM-solver is used, the convergence uncertainty is evaluated as the difference between the solver settings used for the final dosimetric simulations and a less strict setting, e.g., a convergence rate that is larger by one order of magnitude. For FDTD-simulations, the convergence is evaluated according to Clause 7.2.6 of [12]. For perfectly circular coils, the locations of the exposure maxima may vary, which may require that particular measures be taken, such as repositioning the validation points with respect to the maximum location or introducing modifications, such as feedlines, of the coil model that break the circular symmetry.
- 4. Power budget:** The uncertainty due to the power budget applies to full wave simulations only and is evaluated according to Clause 7.2.5 of [12] for FDTD or to Clause 7.2.4 of [13] for FEM.
- 5. Open boundaries:** Open boundary conditions for full wave simulations include the assumption of incident propagating modes. As most WPT models in the scope of this application note can be assumed to operate under near quasistatic conditions (Appendix A.2), the computational domain chosen is not generally large enough for the reactive fields to decay and the propagating modes to be established. The truncation of the reactive fields with open boundary conditions, which can be expected to have an impact on the characteristics of the DUT model, is evaluated by iterative extension of the computational domain until the impact of the open boundary conditions is sufficiently low for consideration in the uncertainty budget.
For the MQS-solver, Dirichlet- or Neumann boundary conditions are available, and as neither of these correctly represents open space, their impact on the uncertainty must also be assessed by iterative extension of the computational domain according to the procedure described in Clause 9.3.7 of [1].
- 6. Quasistatic approximation:** If the MQS-solver is used, the fields at the validation points are evaluated with a full wave simulation of the DUT model. If this is not possible due to computational limitations, a simplified DUT model that has the same *outer* dimensions of the transmit and receive coils as well as the housing may

be substituted for simulation with the MQS- and the full wave-solver. The maximum deviation of the fields at all validation points is reported as uncertainty.

4.3.2 Modeling the Uncertainty for the Incident E- and H-Fields

The modeling uncertainty of the incident E- and H-field, which includes the contributions of the geometry and material parameters of the DUT model, is evaluated according to Table 1.2. Guidance on the evaluation of the uncertainty components is provided below:

- 1. Model parts and geometry:** As mentioned in Section 3.3, the DUT model should be developed on the basis of the original CAD data, and all parts of the CAD model should be included. If the CAD file is incomplete, some parts may have to be identified on the basis of a visual inspection of the DUT; their dimensions must be measured, and their material properties must be estimated. Depending on the characteristics of the parts, particular strategies for the quantification of their impact on the uncertainty may need to be developed. As a conservative approach, the DUT model may be simulated with and without these parts so that the impact of their presence on the incident fields can be quantified.
- 2. Dielectric parameters:** The parameters of the dielectric parts of the DUT are not always well documented. In such cases, the dielectric parameters should be based on typical parameters of the materials and be varied according to worst-case assumptions. Their impact on the H-field can generally be assumed to be small or even negligible, whereas their impact on the E-field has to be considered for model validation and uncertainty evaluation.
- 3. Ferrite parameters:** The parameters of the ferrite parts of the DUT may not be well documented. As their impact on both the electric and magnetic fields is relevant, these should be based on typical parameters of the materials and be varied according to worst-case assumptions for model validation and uncertainty evaluation unless documented parameters are available.
- 4. Positioning of transmit and receive coils:** The impact of uncertainties in the positioning of the transmitter and receiver of the WPT system is assessed by modifying the distance between these components and the offsets according to the positioning accuracy with respect to the experimental validation setup (Section 4.3.3).
- 5. Coupling of transmit and receive coil:** For MQS simulations, the uncertainty in the measurements of the currents of the transmit and receive coils is applied. For full-wave simulations, the deviations in the measured and simulated square roots of the power transmission coefficients are applied.
- 6. Exposure sources other than the coils:** Other relevant sources may include tuning elements, e.g., inductances and capacitors. As mentioned above, modeling these as lumped elements may lead to an incorrect representation of the incident fields, as the spatial dimensions of the lumped elements differ from those of the actual source. Currents on the feedlines of the coil, the ground planes, or the shielding elements may also need to be taken into consideration.
- 7. Loading of the coil:** The currents induced in the phantom or exposed body give rise to a difference between the incident H-field with and without a conducting load (Lenz's law). This difference can be assessed, e.g., with the help of measurements of the H-fields or by full-wave simulations of the fields in the phantom compared to free space. The simulations may be performed with a simplified coil model. The phantom should not be larger than the exposed body region for which the exposure is assessed.

4.3.3 Experimental Uncertainty in Incident E- and H-Fields

The experimental uncertainty (Item #1 in Table 1.4) for the validation points, which is composed of the instrumentation uncertainty for both the homogeneous and highly gradient fields as well as – if necessary – extrapolation to the location of the validation points (Item #2 in Table 1.4), must be carefully assessed. In Appendix B, the assessment of the uncertainty is demonstrated when a three axis H-field probe is used. For a probe with a radius of 25 mm, the uncertainty is more than ± 10 dB when an average gradient is assumed for the extrapolation; i.e., the total uncertainty would be larger than 10 dB when such a probe is used for validation. When multiple points are used and gradient information is included, the uncertainty may remain within this order of magnitude. When a gradient probe with a sensor diameter of 5 mm is applied, then the uncertainty is reduced to < 2 dB [14].

4.3.4 Validation Uncertainty

The validation uncertainty, i.e., the total uncertainty of the DUT model, takes into consideration the uncertainty of the numerical and experimental evaluation of the fields at the validation points. The numerical contributions described in Sections 4.3.1 and 4.3.2 can be combined as the total numerical uncertainty (Table 1.3). The validation uncertainty is then evaluated according to Section 4.6.

The validation points encompass the region of maximum exposure where the fields are characterized by high gradients. As mentioned in Section 2, the experimental evaluation of these fields is prone to large uncertainties, which is why the validation uncertainty is generally the dominant component in the uncertainty budget.

4.4 Uncertainty Tables Required for Model Validation

Item	Description	Tolerance (dB)	Distr.	Div.	c_i	Std. Unc. (dB)
1	Mesh resolution		N	1	1	
2	Location of evaluation points within mesh		R	$\sqrt{3}$	1	
3	Convergence		R	$\sqrt{3}$	1	
4	Power budget (FDTD and FEM only)		N	1	1	
5	Open boundaries		R	$\sqrt{3}$	1	
6	Quasistatic approximation (if applicable)		R	$\sqrt{3}$	1	
Combined uncertainty ($k = 1$)						

Table 1.1: Uncertainty budget for the numerical errors in simulating the DUT. The assessment of the contributions of the items is described in Section 4.3.1.

Item	Description	Tolerance (dB)	Distr.	Div.	c_i	Std. Unc. (dB)
1	Model parts and geometry		R	$\sqrt{3}$	1	
2	Dielectric parameters		R	$\sqrt{3}$	1	
3	Ferrite parameters		R	$\sqrt{3}$	1	
4	Positioning of transmit and receive coils		R	$\sqrt{3}$	1	
5	Coupling of transmit and receive coil		N	1	1	
6	Exposure sources other than the coils		N	1	1	
7	Loading of the coil		R	$\sqrt{3}$	1	
Combined uncertainty ($k = 1$)						

Table 1.2: Uncertainty budget of the DUT model. The assessment of the contributions of the items is described in Section 4.3.2.

Item	Description	Tolerance (dB)	Distr.	Div.	c_i	Std. Unc. (dB)
1	Simulation parameters (Table 1.1)		N	1	1	
2	Numerical DUT model (Table 1.2)		N	1	1	
Combined uncertainty ($k = 1$)						
Expanded uncertainty ($k = 2$)						

Table 1.3: Total uncertainty of the DUT model.

Item	Description	Tolerance (dB)	Distr.	Div.	c_i	Std. Unc. (dB)
1	Measured field values (probe specification)		N	1	1	
2	Extrapolation to the Maximum Exposure Location (Appendix B)		N	1	1	
Combined uncertainty ($k = 1$)						
Expanded uncertainty ($k = 2$)						

Table 1.4: Uncertainty budget for the experimental values used for the model validation. The assessment of the contributions of the items is described in Section 4.3.3.

4.5 Determination of the DUT Model Validity

The validity of the DUT model is determined by comparing the measured and simulated fields at the validation points, with consideration of the respective experimental and computational uncertainty, according to the following steps based on Annex H.2 of [1]:

- Normalize the measured and simulated fields to the transmitted power (FDTD or FEM) or the coil currents (MQS-solver).
- Determine the numerical uncertainty U_{sim} (Table 1.3) and experimental uncertainty U_{exp} (Table 1.4) for a free-space evaluation of the H-field and, if applicable, also of the E-field.
- Exclude the experimentally assessed field points that are <5% of the corresponding maximum value.
- At every validation point n , compare the experimental ν_{exp_n} and numerical ν_{sim_n} according to the following expression:

$$E_n = \sqrt{\frac{(\nu_{\text{sim}_n} - \nu_{\text{exp}_n})^2}{(U_{\text{sim}(k=2)} \nu_{\text{sim}_n})^2 + (U_{\text{exp}(k=2)} \nu_{\text{exp}_n})^2}} \leq 1 \quad (1.1)$$

- If $E_n \leq 1$ at every validation point n , the model is validated and can be applied to the dosimetric evaluation. Otherwise, the model must be improved.

Note: The FDTD simulation reproduces the coupling of the transmit and receive coils. Due to numerical and modeling related uncertainties, the resonance frequency is generally shifted, and the coupling factor may differ from that of the actual DUT. Both effects can be expected to have an impact on the amplitude and distribution of the incident fields at the location of the exposed body or phantom. Tuning elements may therefore have to be adapted to improve the agreement of the incident field with the validation measurements (Section 4.3.3). For the MQS-solvers, these considerations are not required.

4.6 Model Uncertainty

If the the developed model is valid, the uncertainty of the model is the larger of the values determined in Tables 1.3 and 1.4.

5 Assessment of the Uncertainty of the Dosimetric Quantities

5.1 General

The following sections describe how the total uncertainty is determined when dosimetric simulations are used to demonstrate the compliance of WPT devices. The total uncertainty is composed of the numerical and the modeling uncertainties of the dosimetric simulations that are defined by validation uncertainty (Section 4.3.4) and in the following section.

5.2 Assessment of Numerical Uncertainty in the Dosimetric Evaluations

The assessment of the numerical uncertainties in the dosimetric evaluations is carried out for a representative subset of the exposure configurations described in Section 3.2. It can be expected that similar configurations yield similar levels of numerical uncertainty, which is why it is not necessary to evaluate the uncertainty for all of the large number of possible configurations. The evaluation may be limited, e.g., to the largest and the smallest anatomical models, one scenario per exposed body region, and/or the upper and lower limits of the frequency and distance ranges. A rationale for the choice of the scenarios included in the uncertainty evaluation will be provided.

The numerical uncertainty of the dosimetric evaluations includes the contributions of the parameters and settings of the numerical solver. It is evaluated according to Table 1.5. The target parameters for Table 1.5 are the uncertainties in the evaluation of the induced fields in terms of the applied basic restrictions. Guidance on the evaluation of the uncertainty components is given below:

- 1. Mesh resolution:** The mesh resolution uncertainty is evaluated according to Clause 9.3.2 of [1]. The specified modifications of the mesh resolution should be restricted to the region within which the phantom or body model is located. It should be noted that these modifications may also affect the discretization of the DUT model when a Cartesian mesh is used in the simulations. These modifications are assumed to be covered in the uncertainty of model validation because they lead to a further refinement of the discretization of the DUT model.
- 2. Convergence:** The convergence uncertainty can be evaluated for any given item listed in Section 4.3.1 by replacing the evaluation of the incident field with the applicable dosimetric quantity.
- 3. Power budget:** The uncertainty due to the power budget applies to full wave simulations only and is evaluated according to Clause 7.2.5 of [12] for FDTD or to Clause 7.2.4 of [13] for FEM.
- 4. Open boundaries:** The contribution of the uncertainty of the open boundary conditions can be evaluated for any given item listed in Section 4.3.1 by replacing the evaluation of the incident field with the applicable dosimetric quantity. Only the boundary conditions close to the phantom or body model need to be modified.
- 5. Quasistatic approximation:** The contribution of the uncertainty of the quasistatic approximation conditions can be evaluated for any given item listed in Section 4.3.1: the phantom or body model is included in the simulations, and the evaluation of the incident field is replaced with the applicable dosimetric quantity.

5.3 Assessment of Modeling Uncertainty of the Dosimetric Quantities

As described in Section 5.2, the assessment of the modeling uncertainties of the dosimetric evaluations is carried out for a representative subset of the exposure configurations. The modeling uncertainties include the dielectric parameters, positioning uncertainties within the mesh, the representativeness of the exposure scenarios, and possible shortcomings of the averaging algorithms. Guidance on the evaluation of these uncertainty components is given below:

- 1. Dielectric tissue parameters:** For simulations with anatomical models, the impact of the tissue dielectrics are assessed by means of combinations of their maximum and minimum conductivities and permittivities as outlined in Clause 7.2.7 of [12]. When the MQS-solver is used, only the conductivity is considered for the computation of the induced fields, and the permittivity has no impact on the dosimetric results. For full-wave simulations, the uncertainty of the tissue permittivity is expected to be small. For simulations with the standard phantom, the dielectric parameters of the TSL are specified in [1]. Hence, their contribution to the uncertainty is zero.
- 2. Positioning:** For simulations with Cartesian meshes, the phantom or body model is shifted by \pm one mesh step at the location of the highest field gradient, which is generally at the closest distance from the DUT. Details can be found in Clause 7.2.2 of [12]. For tetrahedral meshes, this uncertainty parameter can be assumed to be zero (Clause 7.2.1 of [13]).
- 3. Representativeness of the exposure scenarios:** The configurations involving anatomical models must be based on worst-case conditions for realistic scenarios, i.e., the smallest possible distance between the DUT and the tissue. The cumulative or probability distribution function of the dosimetric results are determined. For Gaussian distributions, the uncertainty corresponds to the standard deviation, and the sample size corresponds to the number of degrees of freedom.
- 4. Averaging algorithms:** At present, no verification of the averaging algorithms for the calculation of exposure in terms of the basic restriction specified in Annex H.1.4 of [1] is available. Reference results will be based on contributions of the working group members of JWG 63184 of IEC TC106. The uncertainty of the averaging algorithms should therefore be determined on the basis of the variations of the available reference results.
It should be noted that [2] requires the evaluation of the unaveraged maximum local E-field. The uncertainty of this value is assumed to be covered by the evaluation of the discretization uncertainty (Section 5.2).

5.4 Assessment of the Total Uncertainty Budget

The evaluation of the total uncertainty budget in Table 1.7 includes the results of the uncertainty budgets of the dosimetric evaluations (Tables 1.5 and 1.6), as well as the uncertainty of the DUT model (Section 4.6).

Item	Description	Tolerance (dB)	Distr.	Div.	c_i	Std. Unc. (dB)
1	Mesh resolution		N	1	1	
2	Convergence		R	$\sqrt{3}$	1	
3	Power budget (FDTD and FEM only)		N	1	1	
4	Open boundaries		R	$\sqrt{3}$	1	
5	Quasistatic approximation		R	$\sqrt{3}$	1	
Combined uncertainty ($k = 1$)						

Table 1.5: Uncertainty budget for the numerical parameters of the dosimetric simulations. The assessment of the contributions of the items is described in Section 5.2.

Item	Description	Tolerance (dB)	Distr.	Div.	c_i	Std. Unc. (dB)
1	Dielectric tissue parameters		R	$\sqrt{3}$	1	
2	Positioning		R	$\sqrt{3}$	1	
3	Representativeness of the exposure scenarios (ν_3 corresponds to the number of scenarios, the other $\nu_i \rightarrow \infty$)		N	1	1	
4	Averaging algorithms		N	1	1	
Combined uncertainty ($k = 1$)						

Table 1.6: Uncertainty budget for the numerical parameters of the dosimetric simulations. The assessment of the contributions of the items is described in Section 5.3.

Item	Description	Tolerance (dB)	Distr.	Div.	c_i	Std. Unc. (dB)
1	DUT Model (Table 1.4 or Table 1.3 whatever is larger)		N	2	1	
2	Numerical uncertainty of the dosimetric evaluation (Table 1.5)		N	1	1	
3	Modeling uncertainty of the dosimetric evaluation (Table 1.6)		N	1	1	
Combined uncertainty ($k = 1$)						
Expanded uncertainty ($k = 2$)						

Table 1.7: Total uncertainty budget of the dosimetric evaluation.

Note: The total uncertainty budget of the dosimetric evaluation cannot be smaller than the measurement uncertainty of the field at the location of maximum exposure.

6 Conclusions

This application note describes the best practice for the numerical assessment of the exposure to WPT systems operating at frequencies between 1 kHz and 30 MHz. It amends the procedures specified in the current draft of [1] with particular focus on the model validation and the evaluation of the uncertainty of the numerical DUT model. Furthermore, additional guidance with respect to the specifications of [2, 3] is provided.

A Computational Solvers

A.1 General

According to IEC 63184 [1], different field-solvers can be used for computational compliance testing. [1] requires the application of a verified implementation of the computational software. For the verification of the software based on the FDTD, IEC/IEEE 62704-1 [12] is referenced; for FEM, IEC/IEEE 62704-4 [13] is applicable. These standards specify the benchmark tests to be used to demonstrate the technically correct implementation of the computational algorithms and the post-processing algorithms to be used for the evaluation of the psSAR. Benchmark tests for the verification of the algorithms to calculate the spatially averaged induced current density [15] and E-fields [16, 17] as well as for the verification of magnetostatic solvers are specified in IEC 63184 [1]. For other computational techniques, no standardized verification methods are available. Reference problems for the validation of other techniques may be found in [18].

A.2 Quasistatic Limit

The quasi-static solvers neglect the mutual coupling of E- and H-fields and can therefore be applied only under limitations on the frequency and/or the spatial extension of the problem to be simulated. In general, the quasistatic approximation of Maxwell's equations is applicable when the following condition is fulfilled:

$$(2\pi f_0)^2 |\hat{\epsilon}_1| \mu_1 l_0^2 \ll 1$$

where f_0 is the operation frequency of the DUT, $\hat{\epsilon}_1$ is the absolute value of the maximum electric permittivity (which is generally a body tissue), μ_1 is the maximum magnetic permeability (which is generally ferrite), and l_0 is the maximum spatial dimension of the problem to be simulated.

A.3 Selection of a Numerical Solver

For the simulation of WPT systems operating at frequencies of up to 30 MHz with Sim4Life, the FDTD solver or the magneto quasicstatic (MQS) solver can be applied. The following solver properties should be taken into account when selecting the solver:

FDTD and FEM:

- Both E- and H-fields are calculated in the time-domain on a Cartesian mesh.
- Complex spatial distributions of dielectric and magnetic materials and of conductors can be specified including, e.g., the elements of the DUT casing and shielding materials, such as ferrites.
- **FDTD only:** The integration of anatomical body models with high spatial resolution and complex tissue distribution in the Cartesian mesh of the method is straightforward, and, in general, a local mesh resolution of better than 1 mm is possible, e.g., in body regions with high exposure.
- **FEM only:** The integration of anatomical body models with a large number of complex tissue shapes and thin layered structures in a tetrahedral mesh that lead to excessive memory requirements may require certain simplifications of the anatomical model.
- A large number of different materials, e.g., the tissues of an anatomical body model, do not lead to significant computational penalties.
- Modeling of dielectric, magnetic, and conducting losses is possible but may not necessarily be required.
- The DUT can be fed with a lumped source that is part of the DUT model, i.e., with a current or voltage source specified on a mesh edge.
- Tuning and loading elements, e.g., capacitors, resistors, and inductors, can be integrated into the model.
- Currents induced, e.g., in coupled coils or in dielectric loads, e.g., the exposed body, are calculated.

- Parameters, e.g., the feedpoint impedance, can be evaluated for a broad frequency range. E- and H-fields can be calculated at multiple frequencies with a single simulation.
- The power budget is available for validation of the simulation results.
- The simulation times, in particular for FDTD, may be large for highly resonant structures.

MQS:

- The MQS-solver is used to calculate the E-field induced by an incident H-field in the frequency domain. For quasistatic WPT-applications, only the E-field due to conduction currents is taken into consideration.
- The MQS-solver can be applied only when it can be demonstrated that the exposure to the E-fields of the DUT is negligible in comparison to the exposure to the H-fields.
- The E-field is calculated only in the phantom or anatomical body model. It is a function of the incident H-field, the frequency and the spatial distribution of the electric conductivity of the TSL or the biological tissues.
- The incident H-field is modeled independently from the simulations of the MQS-solver. If the DUT has no parts with a relative permeability other than 1, the incident H-field can be calculated with a Biot-Savart-Solver. If the DUT contains electrically conducting or ferrite parts, the incident H-fields must be calculated with the Magnetostatic Vector-Potential Solver.
- The displacement currents and the coupling of both the displacement currents and the conduction currents with the incident H-field are not taken into account. Hence, static solvers can be used to calculate the incident H-field as described above.
- The coil currents have fixed amplitudes that need to be set before the simulations. Coupling between two coils is not accounted for, i.e., the currents in coupled coils must be known before the incident field is calculated.
- As the E-field is not calculated, the power budget, the feedpoint impedance or other S-parameters cannot be evaluated.

B H-Field Decay Along the Body Surface

The field gradient uncertainty depends on the method applied by the measurement system to evaluate the field gradient. Common three axis probes that integrate the field over a large surface given by their pick-up loops and do not appropriately capture the maximum fields at the smallest possible distance from the DUT. These may not be specified for measurements at close distances (see, e.g., Clause 7.1.7.1 of [2]) and can be assumed to be prone to significant uncertainties when fields with high gradients are measured.

For the evaluation of a set of example cases, Figure 3 shows a probe with three pick-up loops measuring the H-field at distance d above the cover of a WPT system. The deviation of the measured field integrated over the areas of the three loops from the actual H-field maximum at the cover of the WPT system for the 70 different generic WPT coils evaluated in [19] is given in Figure 4 as a function of the probe diameter. The errors of the 70 different cases is normalized to the mean value for their respective radii. The mean values are given as figures in the plots below the respective error distributions. The deviations of a gradient probe, which uses a pick-up loop with 5 mm radius for the measurements of surface fields are given for comparison [19]. This has already been evaluated by [2]. [2] requires a measurement distance of $1.7 \times$ the probe diameter, which greatly reduces the uncertainty of the measurements but does not allow evaluating the exposures closer than this distance with reasonable uncertainty.

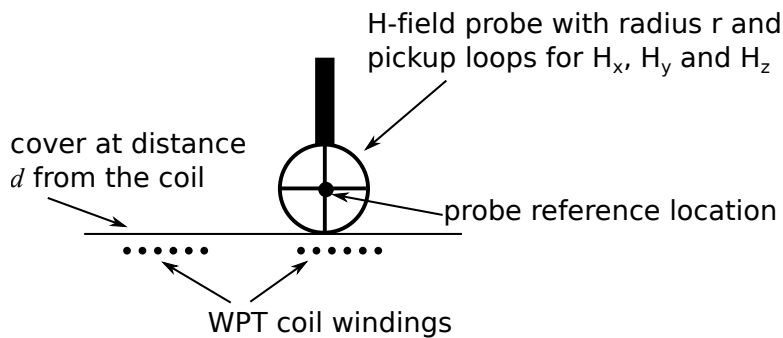


Figure 3: H-field probe with pickup loops of radius r for the three vector components above the windings of a WPT coil. The probe tip touches the cover of the WPT system and is located at distance d from the coil. The probe reference location is in the probe center at the distance $d + r$.

The results shown in Figure 4 demonstrate that the uncertainty of the H-field measured by three-axis probes with large pick-up loops increases as a function of the probe diameter. For a diameter of 100 mm, the uncertainty can exceed 20 dB. The deviations of the gradient probe are within 2 dB for the evaluated coils.

Figure 5 shows the magnitude of the H-field for a subset of the 70 generic WPT coils shown in Figure 4 [19] as a function of the height above the coil at different distances from the center axis, normalized to the value at distances between 20 mm, 40 mm, and 50 mm. For a normalization distance of 20 mm, the maximum fields at the DUT surface are about 35 dB higher than the value at 20 mm. At the larger normalization distances of 40 mm and 50 mm, the maximum fields at the DUT surface are as much as 50 dB greater than the value at the normalization distance. The fields at distances larger than the normalization distance are within the same order of magnitude for 40 mm and 50 mm. In conclusion, it is not possible to predict the slope of the field gradient from measurements at the larger normalization distances. Extrapolation of the maximum field at positions close to the WPT coil is therefore always prone to uncertainty. Figure 5 illustrates that, for fields that decay rapidly from the source, the source model cannot be validated at large distances, because the different field configurations are similar at larger distances. This conclusion is made clear by the small spread of the curves at the end of the z -axis in the plot for normalization at 50 mm while having largely different exposure fields at the surface of the DUT, as shown by the large spread at $z = 0$ in the same plot. This uncertainty increases with the distance of the probe from the surface as well as with the probe diameter.

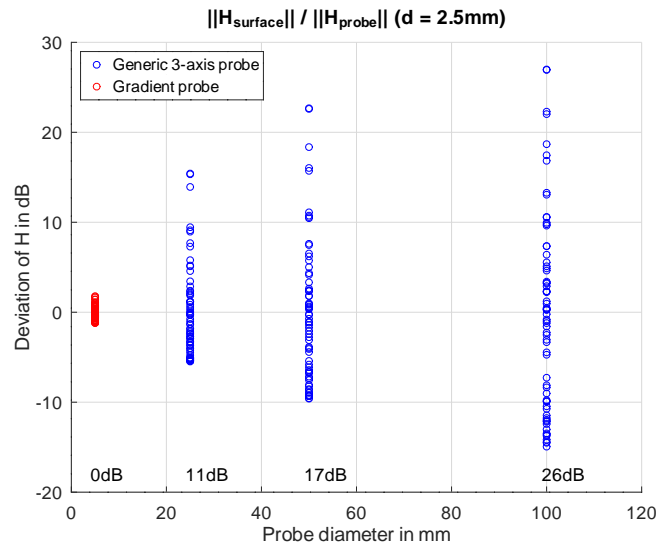


Figure 4: Deviation of H-field $\|H_{\text{surface}}\|$ at the surface of the DUT from the readout $\|H_{\text{probe}}\|$ when determined with probes having diameter d (Figure 3) at $d = 2.5$ mm above 70 different generic WPT coils [19], with the mean decay value used ofr extrapolation. The uncertainty is 10 dB for a diameter of 25 mm and 20 dB for a diameter of 50 mm. The uncertainty can be reduced to 2 dB only for probe diameters <10 mm when measured gradient information is used.

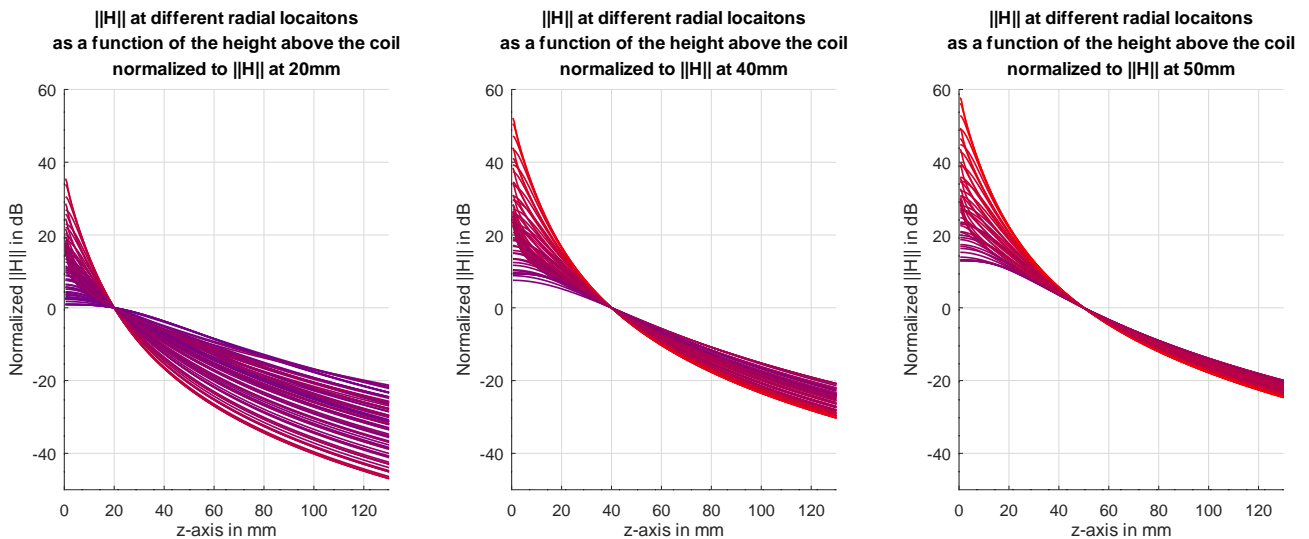


Figure 5: The magnitude of the H-field for a subset of the 70 generic WPT coils shown in Figure 4 [19], as a function of the height along the z-axis above the coil at different distances from the center axis, normalized to the value at distances of 20 mm, 40 mm, and 50 mm.

C Sample Evaluation of an 85 kHz Source with MAGPy

The objective of this Appendix is to provide a sample evaluation for a 85 kHz source based on simulations. The source consists of a 13-turn oval-shaped coil with outer and inner dimensions of 350 mm×200 mm and 314 mm×164 mm, respectively. The measurements for the validation of the numerical DUT model were made with a MAGPy probe according to the guidance presented in Section 4. In Appendix D, a probe with a diameter of 50 mm was used instead in the model validation measurements.

In the first step, we experimentally validated whether the incident E-field could be neglected. We searched for the location of the maximum incident E-field at a distance of 30.5 mm relative to the top sunface of the source casing and determined the E/H ratio based on the incident E-field (33.2 V/m) and H-field (25.1 A/m) measured there. The E/H ratio at the maximum E-field location at 30.5 mm distance was 1.32 Ω , much smaller than the free-space wave impedance 377 Ω . Also we confirmed that the local E-field – induced by the overall maximum incident E-field measured and compensated for the worst-case underestimation of 23 dB (4270 V/m, derived by scaling up the measurement value 302 V/m by 23 dB (see [19]) – was much smaller than that induced by the incident H-field (169 A/m) measured there. The E-fields induced by the incident E- and H-fields were estimated with the capacitive coupling formula and the generic gradient source model, respectively, (both implemented in MAGPy). Since the incident E-field can be neglected and the source is electrically small at 85 kHz, the source could be evaluated by means of MQS simulations.

The DUT model of the source was developed on the basis of its CAD model, as shown in Figure 6. The uncertainties, i.e., U_{sim} and U_{exp} , used to validate the DUT model are provided in Tables 8 and 9, respectively. Among the uncertainty components for U_{sim} , many of them are not applicable or could be neglected because of the simple composition of the evaluated coil (e.g., no dielectric, metallic, or ferrite parts) and application of the MQS solver. The uncertainty of the mesh resolution was evaluated by checking the variation in the field results after refining the resolution by a factor of 2 across all axes. The uncertainty of the evaluation point location was evaluated by comparing the fields directly calculated for a given grid and those interpolated to that grid. The uncertainty of the quasistatic approximation was determined by comparing the results from MQS and FDTD simulations. The uncertainty of the source current was estimated from an analysis of its measurement results. A MAGPy handheld system was used in the model validation measurements, so details about U_{exp} can be found in the MAGPy manual [19]. The DUT model could be validated successfully, as shown in Table 10.

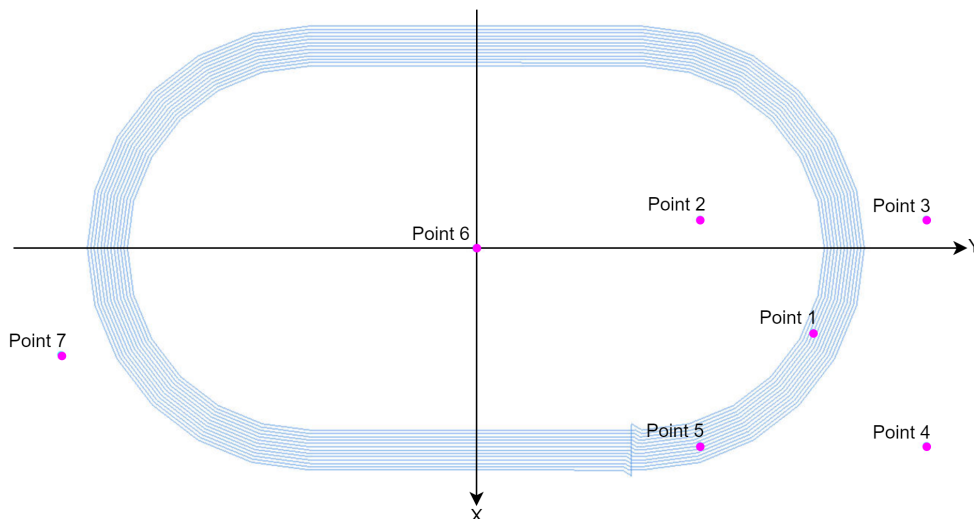


Figure 6: DUT model of the 85 kHz source used in the MQS simulations, showing the validation points. The coordinates of the validation points are provided in Table 10. Point 6 coincides with the coil center. The top surface of the source lies at $z = 0$, so the z -coordinate is equal to the relative distance to the source.

Simulation results of the peak induced fields in a homogeneous phantom filled with TSL ($\sigma = 0.75 \text{ S/m}$, $\rho = 1000 \text{ kg/m}^3$) and positioned at 2 mm from the source are provided in Table 11. The total uncertainty of the induced field values is provided in Table 12. Among the uncertainty components for the total uncertainty budget of the dosimetric evaluation, U_{exp} was adopted as the uncertainty of the DUT model since $U_{exp} > U_{sim}$. The uncertainties for dielectric tissue parameters and the representativeness of the exposure scenarios are not applicable since the evaluation made was based on a homogeneous phantom having standardized tissue properties [1]. The positioning uncertainty was evaluated by checking the variation in the induced fields by changing the phantom-to-source distance by 0.25 mm. Other uncertainties were determined similarly to those in Table 1.1.

Item	Description	Tolerance (dB)	Distr.	Div.	c_i	Std. Unc. (dB)
1	Mesh resolution	0.10	N	1	1	0.10
2	Location of evaluation points within mesh	0.16	R	$\sqrt{3}$	1	0.09
3	Convergence	< 0.1	R	$\sqrt{3}$	1	0.06
4	Power budget (FDTD and FEM only)	N.A.	N	1	1	0
5	Open boundaries	< 0.1	R	$\sqrt{3}$	1	0.06
6	Quasistatic approximation (if applicable)	< 0.1	R	$\sqrt{3}$	1	0.06
7	Model parts and geometry	N.A.	R	$\sqrt{3}$	1	0
8	Dielectric parameters	N.A.	R	$\sqrt{3}$	1	0
9	Ferrite parameters	N.A.	R	$\sqrt{3}$	1	0
10	Positioning of transmit and receive coils	N.A.	R	$\sqrt{3}$	1	0
11	Coupling of transmit and receive coil	N.A.	N	1	1	0
12	Exposure sources other than the coils	N.A.	N	1	1	0
13	Source current	0.42	R	$\sqrt{3}$	1	0.24
14	Load/Backscattering of the load	0.1	R	$\sqrt{3}$	1	0.06
Combined uncertainty ($k = 1$)						0.30
Expanded uncertainty ($k = 2$)						0.59

Table 8: Uncertainty budget for the DUT model of an 85 kHz source.

Item	Description	Tolerance (dB)	Distr.	Div.	c_i	Std. Unc. (dB)
1	Measured field values (probe specification)	0.56	N	1	1	0.56
2	Extrapolation to the maximum exposure location	1.20	N	1	1	1.20
Combined uncertainty ($k = 1$)						1.33
Expanded uncertainty ($k = 2$)						2.65

Table 9: Uncertainty budget for the measurements used to validate the DUT model of an 85 kHz source. The expanded uncertainty is valid for distances <18.5 mm (since the H-field extrapolation in MAGPy has to be enabled), whereas it decreases to 1.13 dB for distances ≥ 18.5 mm.

Point#	x [mm]	y [mm]	z [mm]	H_{simu} [A/m]	H_{meas} [A/m]	E_n	Remarks
1a	38	152	0	243	214	0.37	H-field max.
2a	-13	101	0	57.2	63.9	0.29	Point surrounding H-field max.
3a	-13	203	0	23.4	34.0	0.87	Point surrounding H-field max.
4a	89	203	0	10.1	7.91	0.76	Point surrounding H-field max.
5a	89	101	0	219	165	0.89	Point surrounding H-field max.
6a	0	0	0	43.1	45.6	0.15	Center point
1b	38	152	20	72.7	72.3	0.04	
2b	-13	101	20	51.4	51.7	0.04	
3b	-13	203	20	20.5	22.6	0.62	
4b	89	203	20	9.73	9.55	0.12	
5b	89	101	20	66.0	66.5	0.05	
6b	0	0	20	40.6	40.9	0.05	
1c	38	152	40	38.2	40.0	0.29	
2c	-13	101	40	40.7	41.1	0.06	
3c	-13	203	40	16.2	17.5	0.49	
4c	89	203	40	8.86	9.25	0.28	
5c	89	101	40	35.4	38.2	0.47	
6c	0	0	40	35.4	35.7	0.06	
7	48	-187	30.5	22.1	25.1	0.79	E-field max. at 30.5 mm

Table 10: Results of the DUT model validation performed with MAGPy V2.4. The validation points were selected according to the guidance in Section 4. Points 6a, 6b, 6c, and 7 are optional. The coordinate system is illustrated in Figure 6. The simulated H-fields were normalized to the source current of 0.8 A before being compared to the measured values. The H-fields measured at the probe tip and the probe center were adopted for distances <18.5 mm (i.e., 0 mm here) and ≥ 18.5 mm (i.e., 20, 30.5, and 40 mm here), respectively. Accordingly, the validation metric E_n was derived with $U_{sim} = 2.65$ dB and $U_{sim} = 1.13$ dB for distances <18.5 mm and ≥ 18.5 mm, respectively.

Peak E_{cube} [V/m]	Peak E_{local} [V/m]	Peak E_{line} [V/m]	Peak J_{area} [A/m ²]	psSAR1g [mW/kg]	psSAR10g [mW/kg]
3.27	3.31	3.31	2.29	7.59	5.51

Table 11: Simulation results of the peak induced fields in the homogeneous phantom with a spacing of 2 mm between the phantom surface and the 85 kHz source, normalized to the source current of 0.8 A. E_{cube} , E_{line} , and E_{local} are $2 \times 2 \times 2$ mm³ cube-averaged, 5 mm line-averaged, and local (i.e., not spatial averaged) induced E-fields, respectively. J_{area} is the 1 cm² area-averaged current density. psSAR1g and psSAR10g are peak values of 1 g and 10 g mass-averaged SAR, respectively.

Item	Description	Tolerance (dB)	Distr.	Div.	c_i	Std. Unc. (dB)
1	DUT Model	3.30	N	2	1	1.65
2	Mesh resolution	0.22	N	1	1	0.22
3	Convergence	0.10	R	$\sqrt{3}$	1	0.06
4	Power budget (FDTD and FEM only)	N.A.	N	1	1	0
5	Open boundaries	0.10	R	$\sqrt{3}$	1	0.06
6	Quasistatic approximation	< 0.1	R	$\sqrt{3}$	1	0.06
7	Dielectric tissue parameters	N.A.	R	$\sqrt{3}$	1	0
8	Positioning	0.20	R	$\sqrt{3}$	1	0.12
9	Representativeness of the exposure scenarios	N.A.	N	1	1	0
10	Averaging algorithms	N.A.	N	1	1	0
Combined uncertainty ($k = 1$)						1.67
Expanded uncertainty ($k = 2$)						3.34

Table 12: Total uncertainty budget of the dosimetric evaluation of an 85 kHz source. The uncertainty of the DUT model corresponds to the larger value of the uncertainties determined in Tables 8 and 9.

D Sample Evaluation of an 85 kHz Source with a 50 mm Probe

If the numerical DUT model of an 85 kHz source were validated by measurements made with a probe having a diameter of 50 mm, U_{exp} ($k=2$) would increase to 20 dB (see Figure 4), leading to a very large total uncertainty of the dosimetric evaluation, as shown in Table 13.

Item	Description	Tolerance (dB)	Distr.	Div.	c_i	Std. Unc. (dB)
1	DUT Model	10.0	N	1	1	10.0
2	Mesh resolution	0.22	N	1	1	0.22
3	Convergence	0.10	R	$\sqrt{3}$	1	0.06
4	Power budget (FDTD and FEM only)	N.A.	N	1	1	0
5	Open boundaries	0.10	R	$\sqrt{3}$	1	0.06
6	Quasistatic approximation	< 0.1	R	$\sqrt{3}$	1	0.06
7	Dielectric tissue parameters	N.A.	R	$\sqrt{3}$	1	0
8	Positioning	0.20	R	$\sqrt{3}$	1	0.12
9	Representativeness of the exposure scenarios	N.A.	N	1	1	0
10	Averaging algorithms	N.A.	N	1	1	0
Combined uncertainty ($k = 1$)						10.0
Expanded uncertainty ($k = 2$)						20.0

Table 13: Total uncertainty budget of the dosimetric evaluation of an 85 kHz source. The total uncertainty is dominated by the uncertainty of the validation measurements with the 50 mm probe.

Bibliography

- [1] IEC 63184-CDV. *DRAFT Assessment methods of the human exposure to electric and magnetic fields from wireless power transfer systems—Models, instrumentation, measurement and computational methods and procedures (Frequency range of 1 kHz to 30 MHz)*. International Electrotechnical Commission (IEC), IEC Technical Committee 106, Geneva, Switzerland, 2022.
- [2] Spectrum Management and Industry Canada Telecommunications, Radio Standards Specification. SPR-002, Issue 2, Supplementary procedure for assessing compliance of equipment operating from 3 kHz to 10 MHz with RSS-102, 2022.
- [3] Federal Communications Commission. FCC KDB 680106 D01 v04, Equipment authorization of wireless power transfer devices, 2023.
- [4] IEC/IEEE 62209-1528. *Measurement Procedure for the Assessment of Specific Absorption Rate of Human Exposure to Radio Frequency Fields from Hand-Held and Body-Worn Wireless Communication Devices: Human Models, Instrumentation and Procedures (Frequency Range of 4 MHz to 10 GHz)*. International Electrotechnical Commission (IEC), IEC Technical Committee 106, Geneva, Switzerland, 2020.
- [5] Marie-Christine Gosselin, Esra Neufeld, Heidi Moser, Eveline Huber, Silvia Farcito, Livia Gerber, Maria Jedsjö, Isabel Hilber, Fabienne Di Gennaro, Bryn Lloyd, et al. Development of a new generation of high-resolution anatomical models for medical device evaluation: the virtual population 3.0. *Physics in Medicine & Biology*, 59(18):5287, 2014.
- [6] Andreas Christ, Arya Fallahi, Esra Neufeld, Quirino Balzano, and Niels Kuster. Mechanism of capacitive coupling of proximal electromagnetic sources with biological bodies. *Bioelectromagnetics*, 43(7):404–412, 2022.
- [7] Schmid & Partner Engineering AG. Application note: Characterization of MAGPy E-Field Sensor. Technical report, January 2024.
- [8] Jingtian Xi, Andreas Christ, and Niels Kuster. Coverage factors for efficient demonstration of compliance of low-frequency magnetic near-field exposures with basic restrictions. *Physics in Medicine & Biology*, 68(3):035007, 2023.
- [9] Andreas Christ, Mark G Douglas, John M Roman, Emily B Cooper, Alanson P Sample, Benjamin H Waters, Joshua R Smith, and Niels Kuster. Evaluation of wireless resonant power transfer systems with human electromagnetic exposure limits. *IEEE Transactions on Electromagnetic Compatibility*, 55(2):265–274, 2012.
- [10] Jagadish Nadakuduti, Mark Douglas, Lin Lu, Andreas Christ, Paul Guckian, and Niels Kuster. Compliance testing methodology for wireless power transfer systems. *IEEE Transactions on Power Electronics*, 30(11):6264–6273, 2015.
- [11] SPEAG. *DASY8/6 Module WPT system handbook, incl. SW module WPT 2.2*. Zurich, Switzerland, 2023.
- [12] IEC/IEEE 62704-1. *Recommended Practice for Determining the Spatial-Peak Specific Absorption Rate (SAR) in the Human Body Due to Wireless Communications Devices, 30 MHz - 6 GHz — Part 1: General Requirements for using the Finite Difference Time Domain (FDTD) Method for SAR Calculations*. International Electrotechnical Commission (IEC), IEC Technical Committee 106, Geneva, Switzerland, 2017.

- [13] IEC/IEEE 62704-4. *Recommended Practice for Determining the Spatial-Peak Specific Absorption Rate (SAR) in the Human Body Due to Wireless Communications Devices, 30 MHz-6 GHz — Part 4: General Requirements for using the Finite Element Method for SAR Calculations*. International Electrotechnical Commission (IEC), IEC Technical Committee 106, Geneva, Switzerland, 2020.
- [14] Schmid & Partner Engineering AG. Application note: Testing WPT with DASY8/6 modules SAR & WPT: Testing compliance with FCC KDB 680106. Technical report, November 2023.
- [15] ICNIRP. Guidelines for limiting exposure to time-varying electric, magnetic and electromagnetic fields (up to 300 GHz). *Health Physics*, 74:494–522, 1998.
- [16] ICNIRP. ICNIRP statement — Guidelines for limiting exposure to time-varying electric and magnetic fields (1 Hz to 100 kHz). *Health Physics*, 99:818–836, 2010.
- [17] IEEE C95.1. *Standard for Safety Levels with Respect to Human Exposure to Radio Frequency Electromagnetic Fields, 0 Hz to 300 GHz*. IEEE Standards Department, International Committee on Electromagnetic Safety, The Institute of Electrical and Electronics Engineers, Inc. 3 Park Avenue, New York, NY 10016-5997, USA, October 2019.
- [18] IEEE 1597.1. *Standard for Validation of Computational Electromagnetics Computer Modeling and Simulations*. IEEE Standards Department, 445 Hoes Lane, P.O. Box 1331, Piscataway, NJ 08855-1331, USA, 2022.
- [19] SPEAG. MAGPy V2.4 Manual, 2024.